

## IX SEPOPE

23 a 27 de maio de 2004  
May, 23<sup>th</sup> to 27<sup>th</sup> – 2004  
Rio de Janeiro (RJ) – Brasil

## IX SIMPÓSIO DE ESPECIALISTAS EM PLANEJAMENTO DA OPERAÇÃO E EXPANSÃO ELÉTRICA

## IX SYMPOSIUM OF SPECIALISTS IN ELECTRIC OPERATIONAL AND EXPANSION PLANNING

SP-049

# Investigating the Possibility of Adverse Dynamic Interaction between Neighbor Secondary Voltage Regulation Areas

Camilo Braga Gomes  
COPPE/UFRJ – CEPTEL

Júlio César Rezende Ferraz\*  
CEPEL

Nelson Martins  
CEPEL

Glauco Nery Taranto  
COPPE/UFRJ

### Abstract

This paper investigates examples of adverse dynamic interaction between neighbor secondary voltage regulation areas.

**Keywords:** Voltage Stability; Coordinated Voltage Control; Mid-Term Simulator; Transient Stability Simulator.

### 1 - Introduction

This paper deals with the coordinated voltage control of generation-transmission networks. This topic is gaining increased interest from the scientific community (both IEEE and CIGRE) and utilities worldwide. By coordinated voltage control we mean a hierarchical control system comprised of primary, secondary and tertiary control levels. The primary control is performed by the voltage regulators of generating plants, synchronous and static condensers, which are usually quite fast. The secondary voltage regulation (SVR) is a slow acting (1 minute response), multivariable and adaptive feedback control that changes the voltage reference settings of the generator exciters in order to promote a generator Mvar scheduling and regulate the transmission system voltage profile. The tertiary voltage control is usually open-loop. It involves the use of an optimal power flow with a customized objective function to provide the operators (at about 15-minute intervals) with suggestions on the optimum changes to the settings of pilot node reference voltages and participation factors (var-sharing) of the reactive power sources.

The different time scales for their responses inherently ensure dynamic decoupling between these three hierarchical levels of voltage control. However, once the same electrical area contains two or more SVRs whose pilot nodes are electrically close, there is a risk of adverse dynamic interaction and instability.

This paper describes the adverse SVR dynamic interactions that may exist in a 10-bus, 4-generator tutorial system having two SVRs. The time domain simulations show the dynamic performance of the tutorial system and the SVRs.

### 2 - Hierarchical Voltage Regulation

Electric utilities in some European countries [1, 2] have adopted coordinated control strategies that maintain an adequate voltage profile at key regions of the system for different loading scenarios. In North America, BPA is investigating various possibilities for transmission-based voltage control [3]. In Brazil, there has been increased interest in investigating the benefits of applying coordinated voltage control schemes [4] at various levels.

Instead of relying only on the experience of the system operators and imposing on them the full responsibility for continuous voltage monitoring and control, voltage regulation at transmission level may be more effectively achieved with more automation and coordination among the reactive control sources. The automatic control of the voltage profile significantly contributes to the enhancement of system security and power quality. The coordinated voltage control resources and actions are organized into three levels, known as “Primary”, “Secondary” and “Tertiary” levels and also a forecast level (referred to as “Forecast Studies”). The primary and secondary levels are closed-loop controls, whereas the tertiary level is generally open-loop, and based on on-line optimal power flow studies.

Figure 1 shows a diagram of the coordinated voltage regulation (CVR) hierarchical structure.

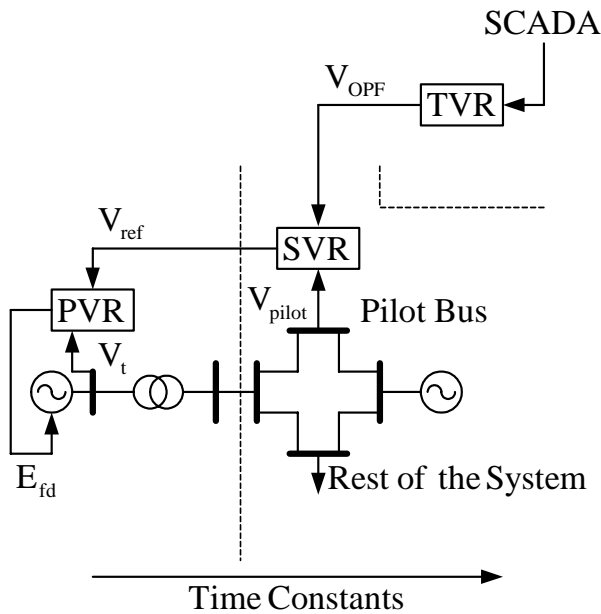


Figure 1 CVR Hierarchical Structure

### 2.1 - Primary Voltage Regulation

Involves fast acting automatic control on individual equipment based on local measurements, with response times ranging from 100 ms up to many seconds. Examples, of fast acting equipment utilized in primary voltage regulation:

- Generators or synchronous compensators with associated voltage regulators (AVR);
- Static var compensators;

Examples of moderately fast to fairly slow equipment utilized in primary control:

- Automatically switched capacitors and reactors banks responding to voltage deviations from nominal values;
- Automatic tap changers;

### 2.2 - Secondary Voltage Regulation (SVR)

The purpose of SVR is to adjust, in real time, manually or automatically, the Primary Control reference points (voltage, reactive power) and to take direct action on various control resources as a function of system requirements.

Actions such as, distribution voltage reductions, tap changer blocking and load-shedding on low voltage are therefore involved. The requirement to minimize the adverse interactions between the primary and secondary controls primary actions and secondary actions, calls for SVR response times larger than one minute.

### 2.3 - Tertiary Voltage and Reactive Power Regulation

This is a relatively slow and manual control (cycle time around 10 minutes or more), which relies on real-time optimal power flow results.

Clearly, tertiary control response time depends on the dispatcher's reaction time (manual control) or the time required for calculating new reference values (computer assisted manual control or automatic). This response time must not be too long (avoiding network conditions that are insecure) or too short (avoiding conflicting actions with the primary and secondary controls).

## 3 - Test System and Control Scheme

### 3.1 - Test System

The test system is shown in Figure 2 and is comprised by 10 buses, 13 lines, 4 generators and two loads. The system data will be described in this section.

The four generators have identical parameters except for the MVA capacity. The generators at buses #1 and #101 are rated 50 MVA while those connected to buses #2 and #102 are rated 150 MVA. Their stator resistances and mechanical damping constants are zero. All lines are purely inductive and their reactances are given in Figure 2. The loads are modeled as constant power. Different values will be assumed for the impedance of the line connecting the two load buses (#30 and #130). This transmission line is the tie-line (intertie) between Area 1 and Area 2 of the test system. As the impedance for this intertie changes in the several power flow cases studied, each case will be named after this parameter ("0.01 pu intertie", for example).

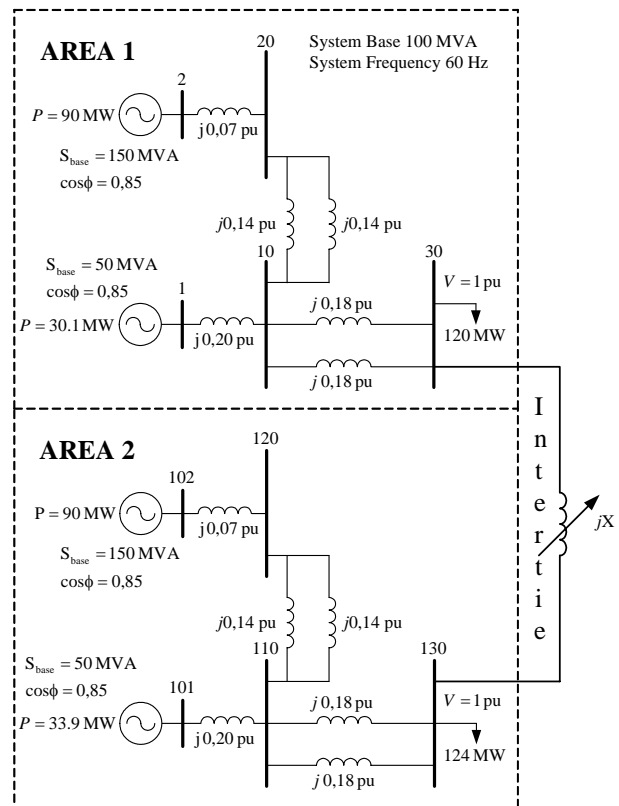


Figure 2 Test System

### 3.2 - Control Scheme

The excitation control system model used in all four machines is shown in Figure 3.

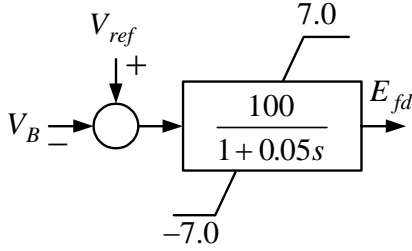


Figure 3 Excitation control system

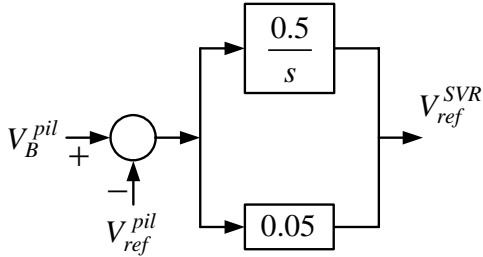


Figure 4 Pilot bus voltage control

Figure 4 shows the block diagram for the pilot bus voltage control. Figure 5 shows the reactive power control for the smaller machines, namely generator #1 and generator #101.

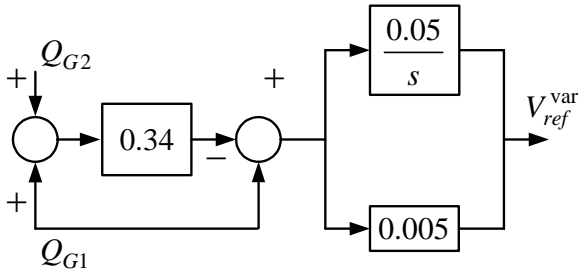


Figure 5 Mvar control for the generators #1 and #101

Figure 6 shows the reactive control for the bigger machines, namely generator #2 and generator #102.

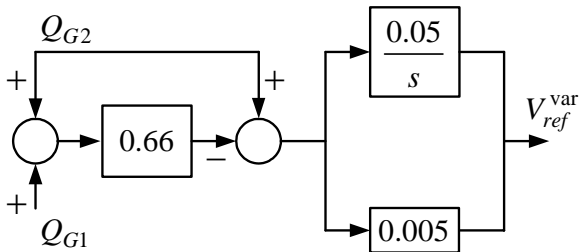


Figure 6 Mvar control for the generators #2 and #102

It is worth noting that when both the pilot bus voltage control and the reactive power control are active, the AVR voltage reference ( $V_{ref}$ ) is the sum of two components, as shown in (1).

$$V_{ref} = V_{ref}^{SVR} + V_{ref}^{var} \quad (1)$$

Reference [5] presents the complete diagram for the secondary voltage regulation system used in each one of the areas of the test system.

The speed-governors are represented in all four generators by the model shown in Figure 7, whose parameter values are  $R = 4\%$  and  $T_G = 0.5$  seconds.

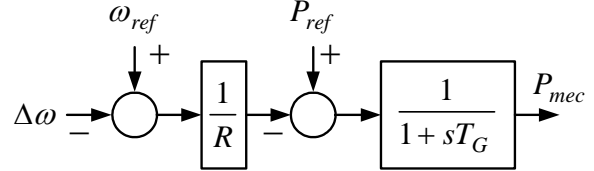


Figure 7 Speed governor

## 4 - Results for the Test System

### 4.1 - Power Flow Program Simulation Results

The power flow program ANAREDE [6] was used to obtain the results shown in this paper. The program FORM CEPEL [7] was used to prepare the power flow tables shown in this paper. These results were obtained for different intertie impedances. The symbols  $P$  and  $Q$  denote active power and reactive power injections respectively.

The tables presenting line power flow results use the following acronyms: Bf (bus from), Bt (bus to), Circ (circuit),  $P$  (active power),  $Q$  (reactive power),  $S$  (apparent power),  $I$  (line current).

Table 1 shows the bus power flow results for a 10 pu intertie. Table 2 shows the line power flow results for the same 10 pu intertie.

Table 1 Bus power flow results for a 10 pu intertie

Bus	Voltage		Generation		Load
	Magnitude (p.u.)	Angle (deg.)	P (MW)	Q (Mvar)	P (MW)
1	1.0217	0.0	30.1	9.0	0
2	1.0217	3.7	90.0	17.1	0
10	1.0058	-3.4	--	--	0
20	1.0118	0.2	--	--	0
30	1.0000	-9.5	--	--	120
101	1.0225	0.0	33.9	9.5	0
102	1.0232	3.3	90.0	18.0	0
110	1.0062	-3.8	--	--	0
120	1.0128	-0.2	--	--	0
130	1.0000	-10.1	--	--	124

**Table 2 Line flows for a 10 pu inertia**

Bf	Bt	Circ	P (MW)	Q (Mvar)	S (MVA)	I (kA)
1	10	1	30.1	9.0	31.4	30.8
2	20	1	90.0	17.1	91.6	89.7
10	20	1	-45.0	-2.9	45.1	44.8
10	20	2	-45.0	-2.9	45.1	44.8
10	30	1	60.1	6.5	60.4	60.1
10	30	2	60.1	6.5	60.4	60.1
30	130	1	0.1	0.0	0.1	0.1
101	110	1	33.9	9.5	35.2	34.4
102	120	1	90.0	18.0	91.8	89.7
110	120	1	-45.0	-3.4	45.1	44.8
110	120	2	-45.0	-3.4	45.1	44.8
110	130	1	61.9	6.9	62.3	61.9
110	130	2	61.9	6.9	62.3	61.9

Table 3 shows the bus power flow results for the 0.01 pu inertia and Table 4 the line power flow results for the 0.01 pu inertia.

**Table 3 Bus power flow results for 0.01 pu inertia**

Bus	Voltage		Generation		Load
	Magnitude (p.u.)	Angle (deg.)	P (MW)	Q (Mvar)	P (MW)
1	1.0221	0.0	32.0	9.2	0
2	1.0224	3.5	90.0	17.5	0
10	1.0060	-3.6	--	--	0
20	1.0123	0.0	--	--	0
30	1.0000	-9.8	--	--	120
101	1.0221	0.0	32.0	9.2	0
102	1.0225	3.5	90.0	17.6	0
110	1.0060	-3.6	--	--	0
120	1.0123	0.0	--	--	0
130	1.0000	-9.8	--	--	124

**Table 4 Line flows for 0.01 pu inertia**

Bf	Bt	Circ	P (MW)	Q (Mvar)	S (MVA)	I (kA)
1	10	1	32.0	9.2	33.3	32.6
2	20	1	90.0	17.5	91.7	89.7
10	20	1	-45.0	-3.1	45.1	44.8
10	20	2	-45.0	-3.1	45.1	44.8
10	30	1	61.0	6.7	61.3	61.0
10	30	2	61.0	6.7	61.3	61.0
30	130	1	2.0	0.0	2.0	2.0
101	110	1	32.0	9.2	33.3	32.6
102	120	1	90.0	17.6	91.7	89.7
110	120	1	-45.0	-3.1	45.1	44.8
110	120	2	-45.0	-3.1	45.1	44.8
110	130	1	61.0	6.7	61.4	61.0
110	130	2	61.0	6.7	61.4	61.0

As shown in Table 2, for a 10 pu inertia there was no power interchange between the two areas. For the 0.01 pu inertia (Table 4) the active power flow was slightly increased (2 MW).

#### 4.2 - Transient Stability Program Results

The transient stability results were obtained with program ANATEM [8], developed by CEPEL. The work reported in this paper investigated conditions that lead to adverse interactions between different secondary

voltage regulation controls. Several simulations were performed on the test system to study this phenomenon. There are two main effects that can be observed in the simulations: one related to the electromechanical phenomena and the other associated with the SVR dynamics. The disturbance was applied after 10 seconds of simulation and chosen so as to excite most the adverse interaction modes between the two SVRs, comprising a positive 5% step at the reference of the SVR controlling the voltage of the pilot bus #30 and a negative 5% step at the reference of the SVR controlling the voltage of the pilot bus #130. The results are shown in the various plots below.

Figure 8 to Figure 12 show the results for the 0.01 pu inertia. Figure 8 shows the unstable voltage oscillations at the pilot bus #30 and Figure 9 shows the unstable voltage oscillations at pilot bus #130.

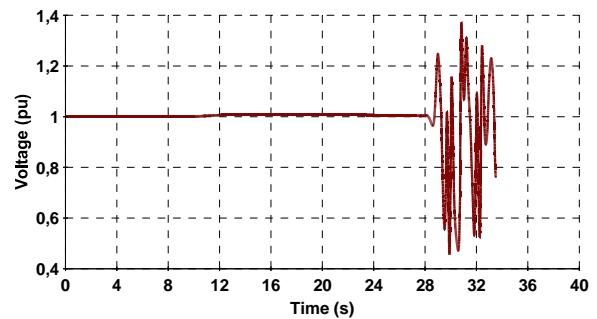
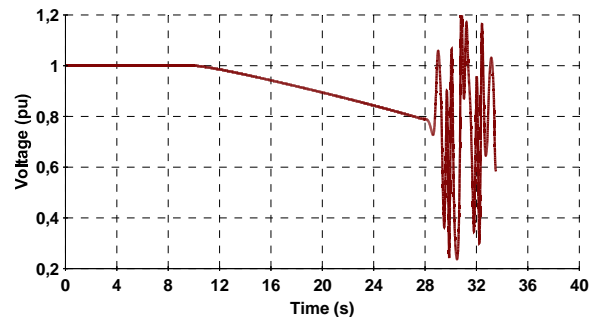
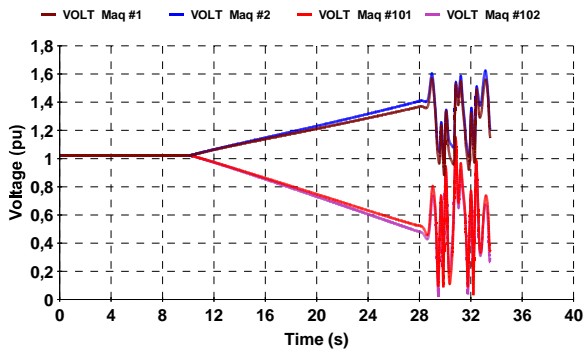
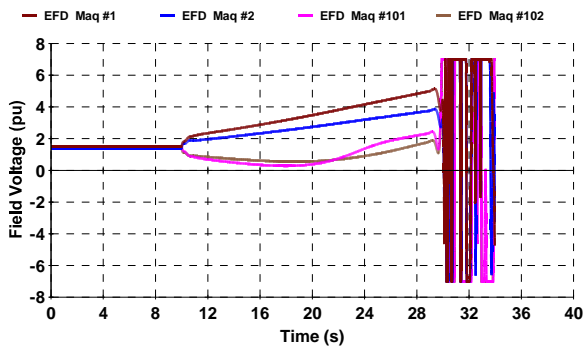
**Figure 8 Voltage at pilot bus #30 (0.01 pu inertia)****Figure 9 Voltage at pilot bus #130 (0.01 pu inertia)**

Figure 10 shows the terminal voltages and Figure 11 the field voltages for all four generators.



**Figure 10 Voltage at generator buses (0.01 pu intertie)**



**Figure 11 Field voltages (0.01 pu intertie)**

Figure 12 shows the active power flowing across the 0.01 pu intertie.

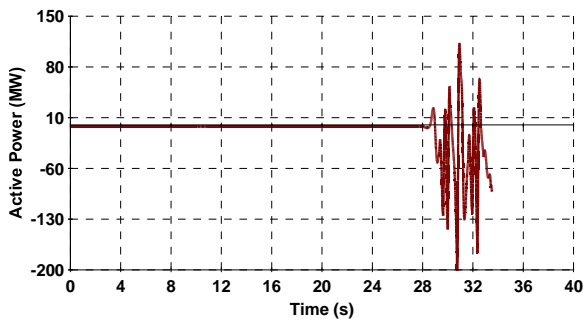


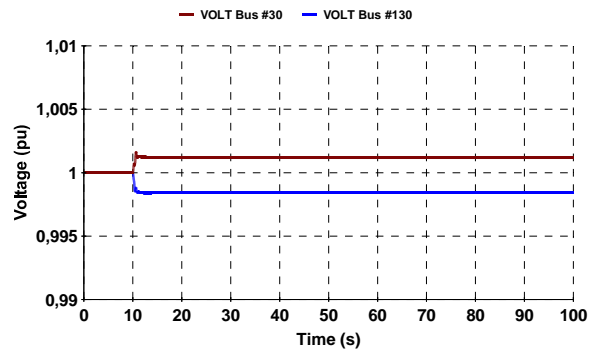
**Figure 12 Active power flowing across the 0.01 pu intertie**

A definite proof that the instability detected in the previous results is related to the adverse interactions between the SVR schemes may be obtained by disconnecting the two SVRs and repeating the simulation.

The following results were performed by turning off both SVR schemes and applying a positive 5% step at generators #1 and #2 and a negative 5% step at generators #101 and #102. The system remained stable, confirming that the cause of the previously detected instability was the adverse interactions between the SVR schemes.

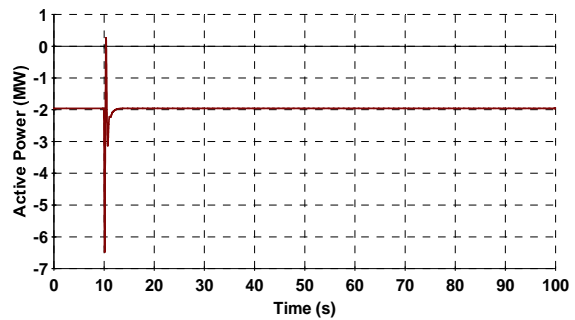
Figure 13 shows the voltages at buses #30 and #130. After the applied disturbance, the voltages do not return

to the initial value since the secondary voltage regulation loops are turned off.



**Figure 13 Voltages at buses #30 and #130 (0.01 pu intertie, no SVRs)**

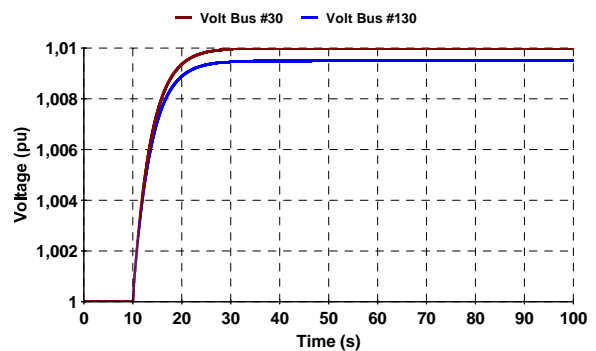
Figure 14 shows the active power flowing across the 0.01 pu intertie.



**Figure 14 Active power flowing across the 0.01 pu intertie (no SVRs)**

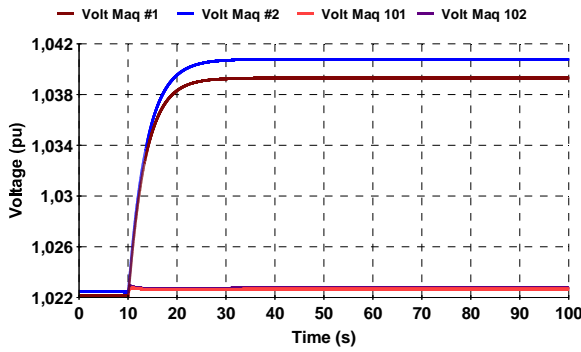
Another proof that instability occurs due to adverse interactions between the SVRs is obtained with simulations for the case where only one SVR (pilot bus #30) is modeled. Figure 15 to Figure 18 show stable results when considering only one SVR.

Figure 15 shows the voltage magnitudes for the pilot bus #30 and the load bus #130, following a positive 1% step at the reference of the SVR for Area 1, controlling the voltage of the pilot bus #30



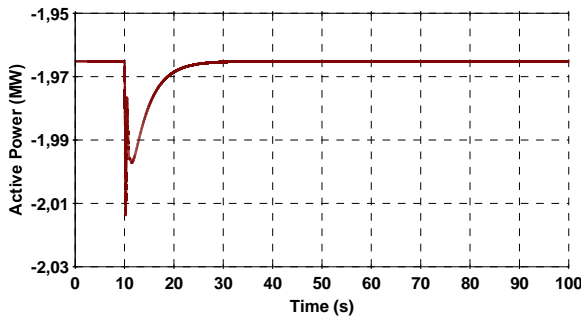
**Figure 15 Voltages at buses #30 and #130 (0.01 pu intertie, no SVR)**

Figure 16 shows the terminal voltages for all four generators.

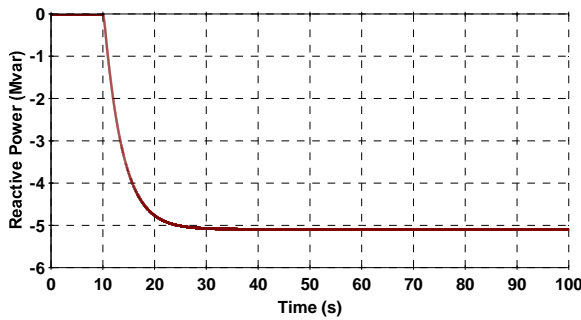


**Figure 16 Voltage at generator buses (0.01 pu inertia)**

Figure 17 and Figure 18 depict the active and reactive powers flowing across the 0.01 pu inertia.



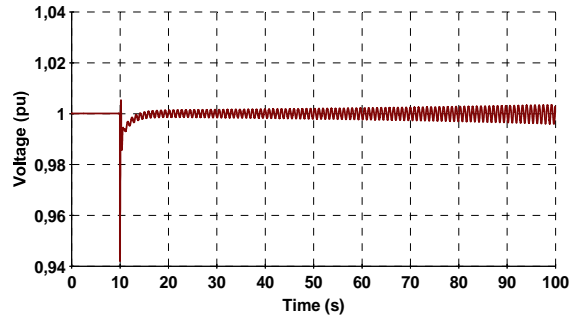
**Figure 17 Active power flowing across the 0.01 pu inertia**



**Figure 18 Reactive power flowing across the 0.01 pu inertia**

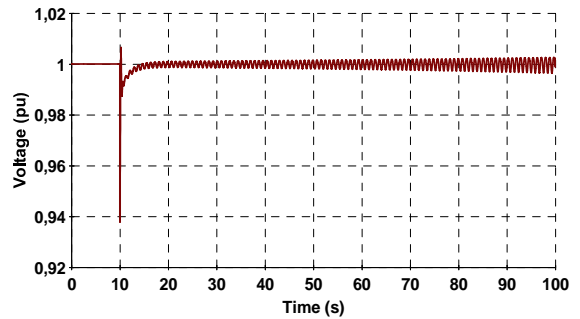
The results shown from Figure 19 to Figure 25 were obtained for a case having a 0.5 pu inertia. The disturbance applied is a 20 MW load increase at bus #30 and a 30 MW load increase at bus #130.

The Figure 19 depicts the voltage of the pilot bus #30 for the system without PSS. It is evident that there is a slightly unstable oscillatory mode. These growing oscillations are, however, not related to the SVR scheme but to an unstable electromechanical mode. When PSSs are added to the system generators, this instability ceases to exist and the system oscillations become well-damped.



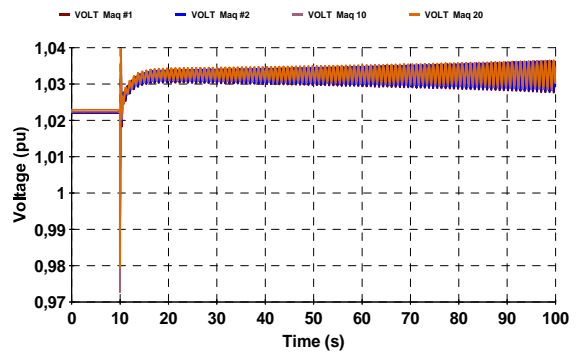
**Figure 19 Voltage at pilot bus #30 without PSS (0.5 pu inertia, no PSS)**

Figure 20 shows the voltage of pilot bus #130 for the system without PSS.



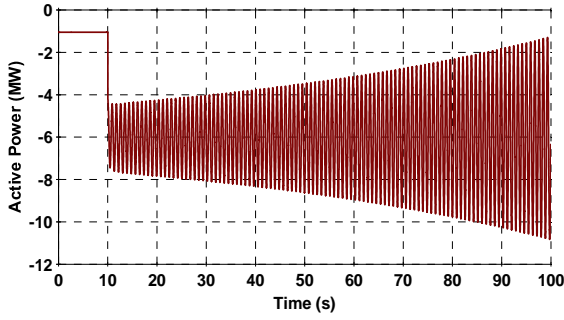
**Figure 20 Voltage at pilot bus #130 without PSS (0.5 pu inertia, no PSS)**

Figure 21 shows the generators terminal voltages for the system without PSS.



**Figure 21 Voltage at generator buses without PSS (0.5 pu inertia, no PSS)**

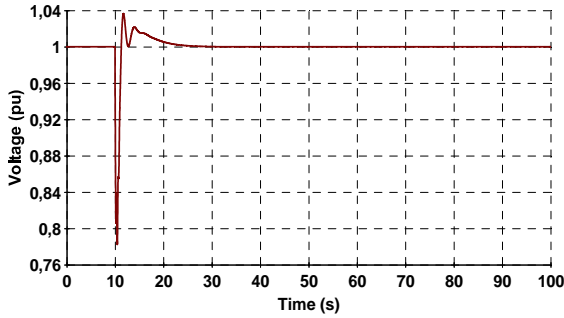
Figure 22 shows the active power that flows across the 0.5 pu inertia for the system without PSS.



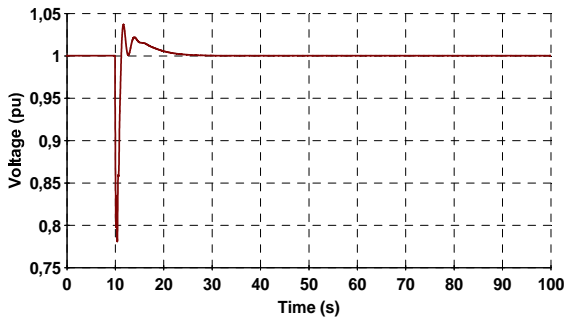
**Figure 22 Active power flowing across the 0.5 pu inertia without PSS**

Figure 23 to Figure 25 show the results for the system with PSSs added to all four generators.

Figure 23 and Figure 24 show the voltages at pilot buses #30 and #130 which now show well-damped oscillations due to the PSS action.



**Figure 23 Voltage at pilot bus #30 (0.5 pu inertia, with PSS)**



**Figure 24 Voltage at pilot bus #130 (0.5 pu inertia, with PSS)**

The Figure 25 shows the active power flowing across the 0.5 pu inertia for the system equipped with PSSs in all four generators.

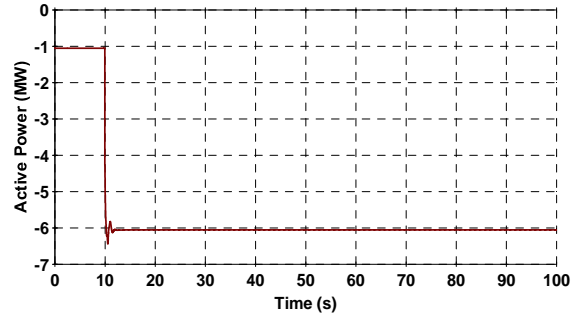


**Figure 25 Active power flowing across the 0.5 pu inertia with PSS**

Other simulations with different applied disturbances were performed, such as load increase and switching shunt devices and the system incorporating the two SVRs proved to be robust and stable.

### 4.3 - Fast Simulation Program Results

The results presented in this section were obtained with an improved version of the fast simulation tool described in [9-11]. This type of simulator [9-11] only captures the mid- and long-term voltage dynamics. The electromechanical dynamics and the fast voltage control dynamics are assumed stable and instantaneous, the final equilibrium point associated with this fast dynamics being represented by a set of algebraic equations. The power system frequency and electromechanical dynamics are neglected. The fairly slow dynamic behavior of the SVR scheme is modeled by differential equations.

The set of nonlinear equations to be solved are given below:

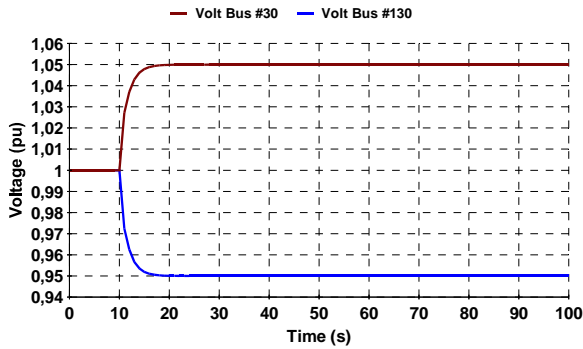
$$\begin{aligned} \dot{y} &= 0 = g(y, x, z, w) \\ \dot{x} &= 0 = f(y, x, z, w) \\ z_d(k+1) &= h_d(y, x, z_d, z_c(k)) \\ \dot{z}_c &= h_c(y, x, z_d, z_c) \end{aligned} \quad (2)$$

Where:

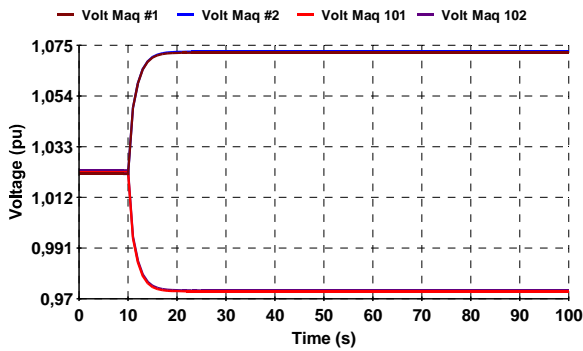
- $y$  Represents the algebraic variables (e.g., bus voltages and angles);
- $x$  Represents the short-term state variables (e.g., machine internal voltages);
- $z_d$  Represents the mid and long-term discrete state variables (e.g., tap position);
- $z_c$  Represents the mid and long-term continuous state variables (e.g., variables associated with the SVR dynamics).

Figure 26 to Figure 29 show results for a 10 pu inertia considering the following disturbance: a positive 5% step at the reference of the SVR controlling the voltage of the pilot bus #30 and a negative 5% step at the reference of the SVR controlling the voltage of the pilot bus #130.

Figure 26 shows the voltages at pilot buses #30 and #130 and Figure 27 shows the voltages at all four generation buses.

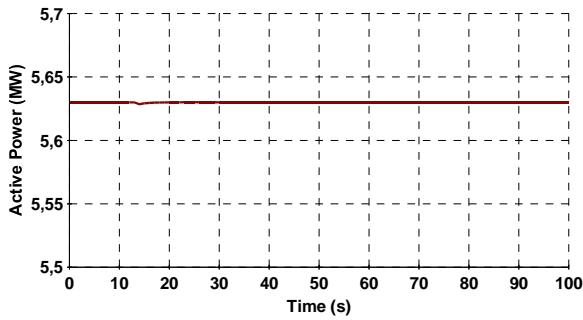


**Figure 26 Voltage at pilot buses #30 and #130 (10 pu inertia)**

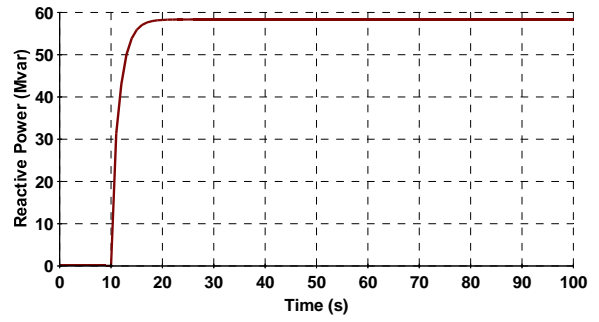


**Figure 27 Voltage at generator buses (10 pu inertia)**

Figure 28 and Figure 29 show, respectively, the active and reactive powers flowing across the tie-line.

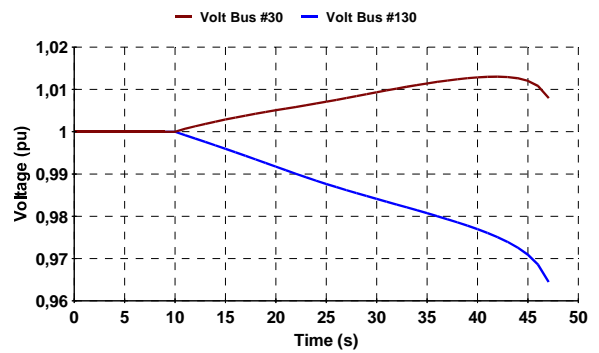


**Figure 28 Active power flowing across the 10 pu inertia**



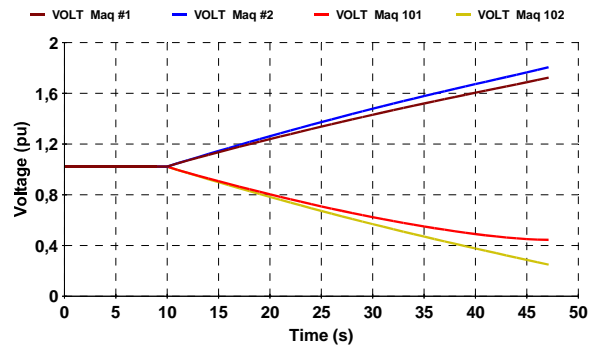
**Figure 29 Reactive power flowing across the 10 pu inertia**

Figure 30 to Figure 34 show results for the 0.01 pu inertia. Figure 30 shows the voltage at pilot bus #30 and the voltage at pilot bus #130.



**Figure 30 Voltage at pilot buses #30 and #130 (0.01 pu inertia)**

Figure 31 shows the terminal voltages and Figure 32 the field voltages for all four generators.



**Figure 31 Voltages at generator buses (0.01 pu inertia)**

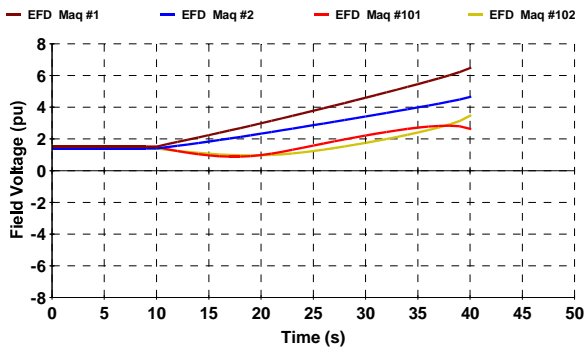


**Figure 32 Field voltage (0.01 pu inertia)**

Figure 33 and Figure 34 show active and reactive powers flowing across the 0.01 inertia.

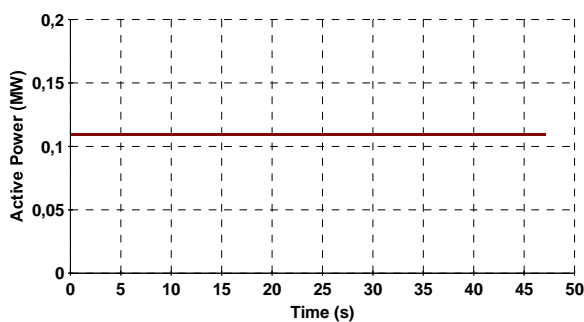


**Figure 33 Active power flowing across the 0.01 pu inertia**

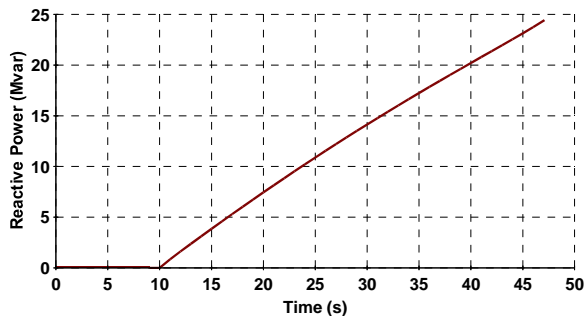


**Figure 34 Reactive power flowing across the 0.01 pu inertia**

## 5 - Conclusions

Attempts to perform independent AGC flat frequency control in the two areas of the test system, without MW interchange control for a 0.01 pu inertia, would similarly result in AGC adverse interactions and possible instability.

By analogy to the MW-interchange control, a Mvar interchange control could also solve the observed instability for the 0.01 pu inertia when having two SVRs. This has been already proposed in [12] but appears not very practical or only to be used in special cases.

The fast simulation tool captured the instability associated with the adverse interactions between the SVRs. This was expected, as the fast simulator adequately models the SVR dynamics.

Results obtained from a transient stability program (ANATEM) and the fast simulator (COPPE/CEPEL Matlab code) showed very good agreement.

Future work will include small-signal analysis (PacDyn) for linearized studies and design of coordinated controls.

## 6 - Bibliography

- [1] **J. P. Paul, J. Y. Léost and J. M. Tesseron**, “Survey of the Secondary Voltage Control in France: Present Realization and Investigations”, *IEEE Transactions on Power Systems*, Vol. 2, No. 2, pp. 505-511, May 1987.
- [2] **S. Corsi, P. Marannino, N. Losignore, G. Moreschini and G. Piccini**, “Coordination between the Reactive Power Scheduling Function and the Hierarchical Voltage Control of the EHV ENEL System”, *IEEE Transactions on Power Systems*, Vol. 10, No. 2, pp. 686-694, May 1995.
- [3] **C. Taylor**, “Line Drop Compensation, High Side Voltage Control, Secondary Voltage Control – Why not Control a Generator like a Static Var Compensator”, *Panel Session on Power Plant Secondary Voltage Control, IEEE/PES Summer Meeting*, Seattle, WA, July 2000.
- [4] **G. N. Taranto, N. Martins, A. C. B. Martins, D. M. Falcão and M. G. dos Santos**, “Benefits of Applying Secondary Voltage Control Schemes to the Brazilian System”, *Proceedings of the IEEE/PES Summer Meeting*, Seattle, WA, July 2000.
- [5] **N. Martins; J. C. R. Ferraz; Sérgio Gomes Jr.; P. E. M. Quintão; J. A. Passos Filho**. A Demonstration Example of Secondary Voltage Regulation: Dynamic Simulation and Continuation Power Flow Results. In: *Power Engineering Society Summer Meeting*, 2001, Vancouver. *Proceedings of Power Engineering Society Summer Meeting*. 2001. v. 2, p. 791-796.
- [6] **CEPEL**, *Programa de Análise de Redes – ANAREDE - Manual do usuário Versão 08-01/03*. Rio de Janeiro, RJ, Brasil, janeiro 2003.
- [7] **CEPEL**, *Programa FORM CEPEL - Manual do usuário Versão 01/2003*. Rio de Janeiro, RJ, Brasil, 2003.
- [8] **CEPEL**, *Análise de Transitórios Eletromecânicos – ANATEM - Manual do usuário Versão 09-12/02*. Rio de Janeiro, RJ, Brasil, dezembro 2002.
- [9] **W. J. Causarano**, *Método de Simulação Rápida no Tempo para Avaliação da Estabilidade de*

Tensão. Tese de M.Sc., COPPE/UFRJ, Rio de Janeiro, RJ, Brasil, 1997.

- [10] **W. J. Causarano, D. M. Falcão and G. N. Taranto**, “A Fast Domain Simulation Method for Voltage Stability Assessment”, *Proceedings of the VI SEPOPE*, Salvador, BA, May 1998.
- [11] **C. B. Gomes**, Implementação de Funções Utilizadas no Controle Coordenado de Tensão num Simulador Rápido. Tese de M.Sc., COPPE/UFRJ, Rio de Janeiro, RJ, Brasil, 2001.
- [12] **M. Tanimoto; Y. Izui; K. Matsuno; N. Fukuta; K. Deno; T. Sasaki**; “An Autonomous Distributed VQC Method Based on Q-TBC”, *Proceedings of the IEEE/PES Summer Meeting*, Seattle, WA, July 2000.